Stopping and storing light coherently

Mehmet Fatih Yanik* and Shanhui Fan
Ginzton Laboratory, Stanford University, Stanford, California 94305, USA
(Received 6 May 2004; revised manuscript received 23 August 2004; published 5 January 2005)

We present a general analysis for the criteria to stop and store light coherently. We show that a light pulse can be stopped in any physical system, provided that (i) the system bandwidth can be compressed to zero; (ii) the system has sufficient degrees of freedom to accommodate the pulse, and the bandwidth compression occurs while the pulse is in the system; and (iii) the bandwidth compression is done reversibly in an adiabatic fashion that preserves the phase space and the information in the original photon pulse during the entire duration of the stopping process. Based upon this general criterion, we present a brief discussion of stopping-light schemes using atomic resonances, and a detailed analysis of the all-optical scheme that we recently proposed. We show that the all-optical scheme can achieve arbitrarily small group velocities for large bandwidth pulses, and opens up new opportunities in both fundamental sciences and technological applications.

DOI: 10.1103/PhysRevA.71.013803 PACS number(s): 42.50.Gy, 42.70.Qs

I. INTRODUCTION

The ability to drastically slow down the propagation speed of light, and to coherently stop and store optical pulses, holds the key to the ultimate control of light, and has profound implications for optical communications [1] and quantum information processing [2–4]. In optical communications, for example, a key function that is currently lacking is the presence of dynamic optical buffering. The ability to stop light could therefore enable far more flexible optical network architectures. In quantum information processing, photons have been a very attractive carrier for quantum information, due to the fact that they interact very weakly among themselves and also with the environment. Consequently, quantum coherence of a photon can be preserved over very long time and distance scales at room temperature. However, the weak photon-photon interaction also introduces a very fundamental problem in quantum information processing, and prevents the realization of a photonic quantum gate unless coherent or resonant light-matter interaction is used [5]. Such use of coherent and resonant light-matter interaction is fundamentally limiting since electronic systems tend to couple to environment strongly. By reducing the group velocity of photons, the interaction time between photons can be dramatically increased for a given propagation distance. This is quite significant as it can enable ultralow power switches and even single-photon quantum gates with the use of only weak nonresonant nonlinearities if photons can be stopped all-optically. Thus, the capability to stop light all-optically could fundamentally alter the outlook of quantum information processing.

To stop light, a necessary requirement is to create a system that can generate small group velocities. Small group velocities can be accomplished with the use of either atomic or optical resonances. Near atomic resonances, the group velocity reduction by many orders of magnitude has been observed [6]. Furthermore, the dissipation of energy due to spontaneous emission and the resulting loss of coherence that typically occur at atomic resonances can be suppressed with quantum interference schemes such as the electromagnetic induced transparency (EIT) [7], Raman assisted interference effects [8], and coherent spectral hole creation [9], leading to coherent atomic states with very long lifetimes. With such techniques, group velocity of light as small as 17 m/s or even less has been demonstrated experimentally [10–14]. On the other hand, with the use of optical resonances in passive dielectric structures, such as the coupled resonator optical waveguides (CROW) [15–17] and the photonic crystal waveguide band edges [18], small group velocities have also been both predicted and demonstrated.

However, having a system with slow group velocity alone is not sufficient to stop light. As we explicitly discuss in this paper, any static resonator system is limited by a fundamental bandwidth-delay product, which constrains the minimum achievable group velocity for the entire bandwidth of optical signals. Consequently, no static resonator system can stop light pulses with a finite and nonzero bandwidth. In the atomic systems, light stopping has been accomplished by the use of dynamic systems in which the optical pulse is transferred (at least partially) to the long-lifetime electronic coherences [19–25]. However, the use of the electronic states has fundamentally limited the applications of stopping light in communications and quantum computing systems. In this paper, we show that the use of electronic coherence is in fact not necessary, and we present an in-depth discussion of the general criterion for stopping light [26] that is applicable to any resonance with atomic, optical, or any other physical origin.

The paper is organized as follows. In Sec. II, we discuss the bandwidth-delay product and the resulting limitations. We then introduce in Sec. III the general criterion that should be satisfied to stop light pulses in any system. This criterion allows one to overcome the constraints imposed by the delay-bandwidth product, and to generate arbitrarily small group velocities for optical pulses. Understanding of such a criterion may thus enable the construction of new systems for stopping light pulses. Based on this general criterion, we discuss in Sec. IV the presently known atomic stop-light

*Email address: fatih@stanford.edu

schemes, as well as the all-optical stop-light scheme we recently introduced. And we conclude with a discussion of possible implications of stopping light all-optically.

II. THE CONSTRAINT OF DELAY-BANDWIDTH PRODUCT: SLOWING LIGHT VERSUS STOPPING LIGHT

The fundamental constraint in any static resonator system is the so-called bandwidth-delay product [27,28]—the group delay from an optical resonance is inversely proportional to the bandwidth within which the delay occurs. For a given resonance, the total phase shift ϕ across the resonance frequency is $m\pi$, where m is the order of the resonance (for a single-mode resonator $m=1$, for an all-pass resonator $m=2$). Thus, we have the following constraint regarding the group delay $\delta t = d\phi/d\omega$:

$$\int d\omega \delta t = \int d\omega \frac{d\phi}{d\omega} = m\pi, \tag{1}$$

where the integration range covers the entire resonant line shape. Thus, the minimum group velocity that is accomplishable by complexes of such resonators is approximately

$$\mathrm{v}_g \approx \frac{L}{\delta\tau} = \frac{L\delta\omega}{m\pi} = \frac{L\delta f}{2m}, \tag{2}$$

where L is the physical length of the resonator. The group velocity a static system can achieve scales linearly with the system bandwidth and the physical dimensions of the resonators. Thus, the group velocity cannot be zero for the entire signal bandwidth unless the signal bandwidth is zero.

More detailed estimates of delay-bandwidth product can be made for specific examples of slow light structures. In a CROW waveguide structure, for example, the minimum group velocity that can be accomplished for pulses at 10 Gbit/s rate with a wavelength of 1.55 μm is approximately 10^{-2} c for minimal distortion. And the corresponding delay one can achieve for a chip size of a few millimeters is less than a nanosecond for a propagation distance of a few millimeters. Similar arguments regarding delay-bandwidth product apply to stationary electronic resonances [29].

Thus, while the use of static resonators can slow down the propagation of light, it cannot bring the group velocity of a light pulse to zero. Stopping light necessarily violates the delay-bandwidth product constraint in static resonator systems. Consequently, stopping light, by definition, requires one to use a dynamic optical system.

III. GENERAL CRITERIA: ILLUSTRATED WITH A ONE-BAND MODEL

To overcome the delay-bandwidth product constraint to stop light, a system must be able to simultaneously satisfy two seemingly contradicting requirements. On one hand, in order for the system to be able to accommodate the entire pulse bandwidth, the bandwidth of the system must necessarily be wide and the group velocity is therefore large. On the other hand, stopping light requires the group velocity to be extremely small, and thus the bandwidth has to be infinitesimally small. The way to satisfy simultaneously such seemingly contradicting requirements is to create a dynamic system where both the system and signal bandwidth change as a function of time such that the following criteria are fulfilled [26]:

(a) The system must possess large tunability in its bandwidth. To allow for an optical pulse with a given bandwidth to enter the system, the system must possess an initial state with a sufficiently large bandwidth, and hence a large group velocity, as required by the delay-bandwidth product [Fig. 1(a)]. To stop the pulse in the system, on the other hand, the group velocity of the pulse needs to be reduced to almost zero. Thus, the system bandwidth should also go to zero for all wave-vector components [Fig. 1(b)].

(b) The tuning of the system needs to be performed in a manner such that the bandwidth of the pulse is reversibly compressed. Such signal bandwidth compression is necessary in order to accommodate the pulse as the system bandwidth is reduced [Fig. 1(b)]. Thus, the tuning process must occur while the pulse is completely in the system, and must be performed in an adiabatic [31] fashion to preserve all the coherent information encoded in the original pulse.

A particularly powerful way to stop light is to use a translationally invariant system [30], and to tune the system in a translationally invariant manner. In doing so, one prevents any scattering in the momentum space, and thus the second condition, which dictates the use of a reversible bandwidth compression process, becomes easier to implement. Any translationally invariant system can be described in terms of a band diagram that relates the frequencies and wave vectors of the eigenmodes, as shown in the bottom panels of Fig. 1. In such a system, a light pulse can be stopped by evolving the system from an initial state, where the slope of the band is large (left panel in the bottom of Fig. 1), to a final state, where the slope of the band is zero (middle panel in the bottom of Fig. 1). The initial state, which has a large system bandwidth, is used to accommodate the entire bandwidth of the signal pulse, with each frequency component of the signal pulse occupying a unique wave vector. In the final state, the group velocity (i.e., the slope) is reduced to zero for all the signal wave-vector components, consequently the system bandwidth is reduced to zero (middle panel in Fig. 1). By performing the process of system bandwidth compression while the photon pulse is in the system, and by doing so in an adiabatic fashion, the signal bandwidth can also be compressed to zero, resulting in the stopping of light without losing any coherent information. The details for adiabaticity depend upon specific systems, and will be discussed specifically in later parts. Here, it is sufficient to point out that the system bandwidth compression process performs a frequency conversion for each wave-vector component of the photon pulse. And by performing this process while preserving the translational invariance, the bandwidth reduction process can preserve the coherent phase information of the original pulse as spatial phase variation even when both the system and the signal bandwidth are reduced to zero.

In practice, all physical systems that have been implemented to stop light involve the use of multiple bands. Such a multiple band system results from the coupling of multiple subsystems in a translationally invariant fashion (Fig. 2).

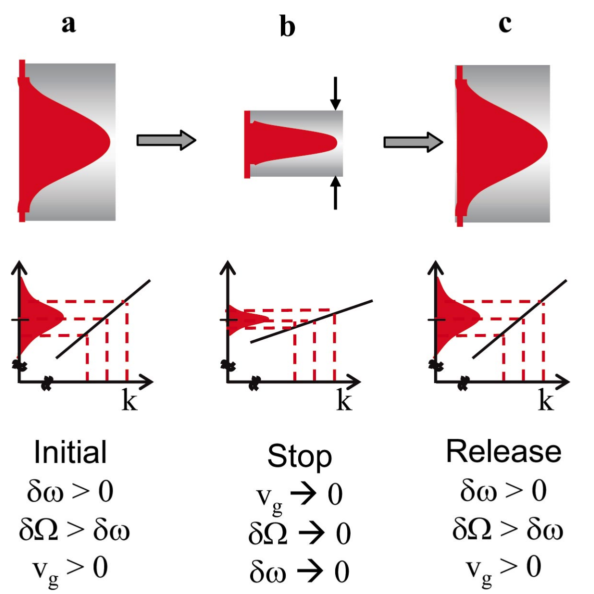

FIG. 1. (Color) Schematic of a one-band model for stopping light. The system and signal bandwidth should be time-dependent. In the top panels, the system bandwidth and the spectral shape of the signal pulse are indicated by the gray block and the filled red curves, respectively. In the bottom panels, the spectral shapes of the pulse are superimposed on the band diagrams of the system. A pulse can be stopped and then released by evolving the system from (a) to (c). (a) The initial state. The system bandwidth (and hence the group velocity) is large in order to accommodate a signal with a given signal bandwidth. (b) The state in which the group velocity is reduced to zero. Here both the system bandwidth and the signal bandwidth are compressed to zero. (c) The final state. The original signal bandwidth and the group velocity are recovered, and the pulse is released with all coherent information preserved. Axes are in arbitrary units.

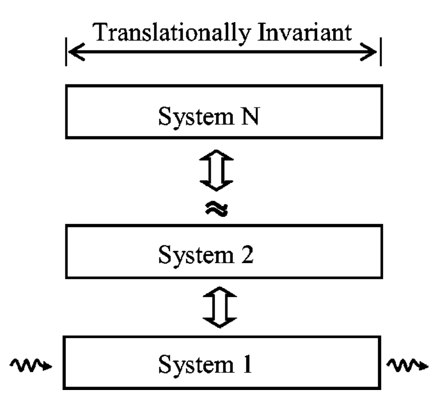

FIG. 2. Schematic for a tunable optical system consisting of several subsystems. Each subsystem has a different characteristic. The subsystems are coupled together in a way that preserves the translational symmetry of the overall system along the propagation direction of photons. By modulating the subsystems, the electromagnetic field can be adiabatically transferred among the subsystems, dramatically changing the spectral properties of both the system and the fields.

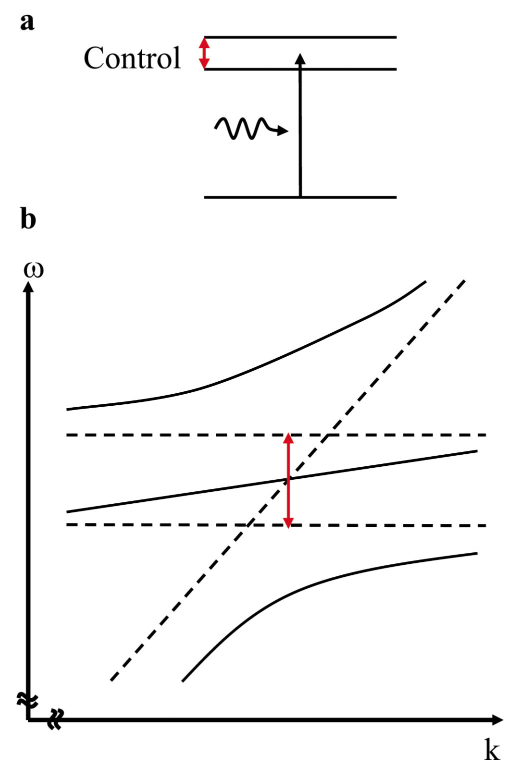

FIG. 3. (Color) Bandwidth compression via modulating dark polaritons, as employed in the EIT stopping light schemes. (a) The externally applied field controls the splitting of the dressed polariton states. (b) The bandwidth of the midband is given by the energy splitting between the dressed states, and can be reduced to zero when the external field is turned off. Axes are in arbitrary units.

Each subsystem can be designed to possess dramatically different optical properties. And by modulating the relative frequencies of the subsystems, the eigenstates of the system can evolve adiabatically between the subsystems, resulting in dramatic changes in optical properties.

Both the electronic stop-light schemes [19–24], and the all-optical scheme we introduced recently [26] can be understood within the framework of such a general system. For instance, in EIT, the system consists of two stationary subsystems of atomic levels and the propagating free-space electromagnetic modes. The coupling between the atomic subsystems induced by an external electromagnetic control field, and the coupling between the atomic systems and the free-space mode, result in the band structure shown in Fig. 3 [32]. By decreasing the strength of the control field, one of the eigenstates (the band in the middle in Fig. 3) adiabatically evolves from propagating free-space optical waves to coherent electronic states, resulting in dramatic compression of the system bandwidth. And a light pulse can be stopped by performing such a process while the entire optical pulse is in the system [19–24].

IV. ALL-OPTICAL IMPLEMENTATION

The use of electronic states to coherently store the optical information, however, imposes severe constraints on the operating conditions and degrades the coherence properties of

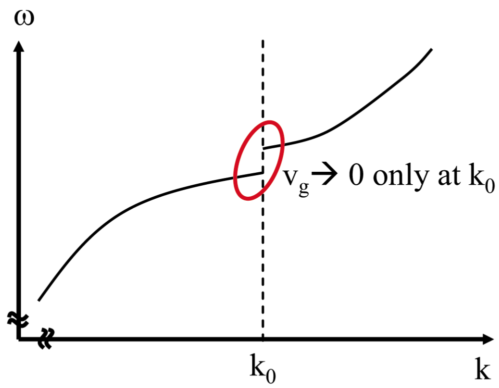

FIG. 4. (Color) Schematic of a band diagram of a one-dimensional photonic crystal. The splitting at the band edge results in group velocity reduction, but only over a narrow wave-vector range. In particular, the group velocity goes to zero only at a single wave-vector component. Axes are in arbitrary units.

photons. Furthermore, only a few very special and delicate electronic resonances available in nature can be used. All the experimentally demonstrated operating bandwidths are far too small to be useful for most purposes. The storage times are fundamentally limited by electronic decoherence processes. The wavelength ranges where such effects can be observed are also very limited. Furthermore, while promising steps have been taken for room-temperature operation in solid-state systems [23,24], it still remains a great challenge to implement such schemes on-chip with integrated optoelectronic technologies at room temperature. Consequently, it is of great interest to pursue the control of light speed using optical resonances in photonic structures including dielectric microcavities [33] and photonic crystals [34–36]. The operation of photonic structures does not require electronic coherences, and is almost completely independent of temperature. Such structures can be defined by lithography and are therefore defined in solid-state systems on-chip, and can operate at any wavelength range of interest.

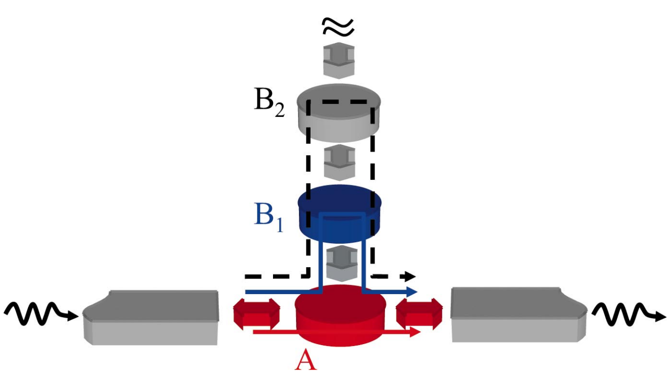

FIG. 5. (Color) The basic building block of the all-optical stop-light system. The disks represent cavities, and the arrows indicate available evanescent coupling pathways between the cavities and the waveguides. A waveguide cavity A is inserted into a waveguide, and one or more side cavities B_i are side-coupled to A. Photons tunnel through multiple pathways indicated by black, blue, and red lines, resulting in Fano interference that is tunable by adjusting the resonant frequency of the cavities.

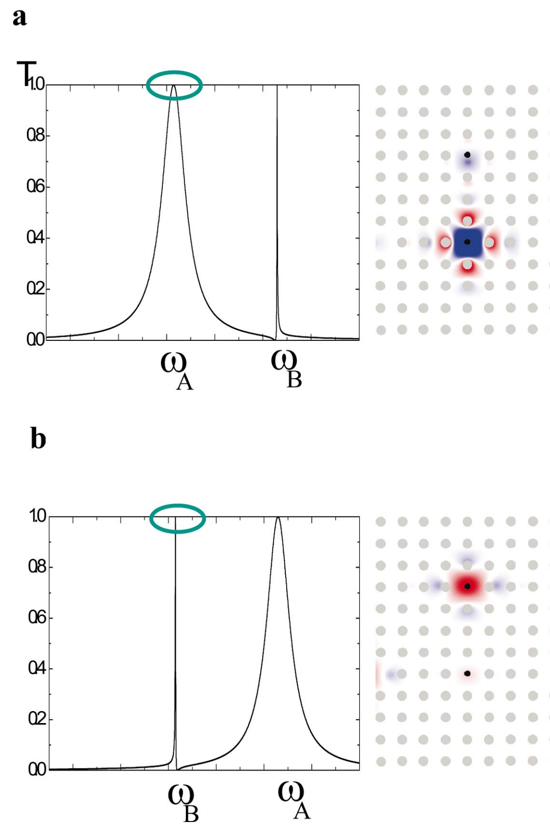

FIG. 6. (Color) Transmission spectra through the system of Fig. 5, but with a single side-cavity B_1. The spectra are calculated for photonic crystal structures shown on the right sides of the figures. The gray dots represent the position of the dielectric rods in a perfect crystal. These rods have a dielectric constant of 11.56 and a radius of $0.2a$, where a is the lattice constant. The black dots represent the cavities with a radius of $0.1a$, and a dielectric constant that is tunable. The field patterns that correspond to the lower-frequency transmission peak are also shown on the right sides. The spectra and the field patterns are for (a) $\omega_A - \omega_B < -|\beta|$ and (b) $\omega_A - \omega_B > |\beta|$, where β is the coupling constant between the cavities. Notice the dramatic variations of the width of the lower-frequency transmission peak as a function of the resonant frequencies.

To tune an all-optical system, the most convenient way is to modulate the refractive index. For transparent materials with low loss, the accomplishable refractive index change is generally quite small ($\delta n/n \approx 10^{-4}$). Consequently, to implement an all-optical scheme for stopping light, one will need to construct special systems in which the bandwidth can be compressed by many orders of magnitude with small refractive index tuning. Many approaches invented for tunable delay or dispersion compensation applications in fact cannot be used. Consider, for example, fiber Bragg gratings, or holographically defined three-dimensional periodic structures. In these systems the group velocity can be reduced to zero at a photonic band edge. For externally incident light, by adjusting either the dielectric constant or the periodicity, the group velocity and the dispersion properties of the system can therefore be tuned. However, in these systems the group velocity would be zero only at a single wave vector (Fig. 4), and yet for stopping light one needs to be able to reduce the group velocity to zero for an entire range of wave vectors. Moreover, the strong dispersion at the band edges can lead to large distortion of the pulses. Similarly, while the bandwidth of a CROW waveguide can in principle be slightly modulated by changing the coupling constants between the microcavities, it is not possible to reduce the bandwidth to zero due to the availability of only limited index modulations.

Guided by the general concepts introduced in the previous section, we implemented a system where arbitrarily large group velocity reduction for all wave vectors can be accomplished with realistic physical constraints [26]. In such a system, arbitrary group velocity reduction can be achieved fast enough before light pulses can pass through the system. And to completely stop light requires only the use of small index modulations ($\delta n/n < 10^{-4}$) performed at moderate speeds 1 -10 GHz, even in the presence of significant losses. The modulation accomplishes a coherent frequency conversion process for all spectral components, and reversibly compresses the bandwidth of the incident pulse by an arbitrarily large amount. Unlike the EIT scheme, however, the propagating electromagnetic field is not transformed to coherent quantum states of electrons, but rather converted to a stationary electromagnetic field distribution.

A. Tunable Fano resonance

In order to construct a system that can change its bandwidth dramatically, we use resonant optical structures that generate sharp tunable resonances through Fano interference. To illustrate the interference process, we consider a basic building block, as shown in Fig. 5, that consists of a resonator A that is directly coupled to a waveguide, and one or more side cavities B_i that are side coupled to the waveguide cavity A. A photon can transmit through this system via multiple pathways, with the spectral characteristics depending strongly on the relative resonance frequencies of the resonators. The presence of such multiple resonance pathways leads to Fano interference [37]. For the case of a single side cavity, the transmission T as a function of the input frequency ω can be derived using coupled-mode theory [38] as

$$T = \left|\frac{S_{out}}{S_{in}}\right|^2 = \left|\frac{\alpha[i(\omega-\omega_A)+\gamma_A]}{-(\omega-\omega_A)(\omega-\omega_B)+\beta^2+\gamma_A\gamma_B+i[(\omega-\omega_B)\gamma_A+(\omega-\omega_A)\gamma_B]}\right|^2, \tag{3}$$

where S_{out} and S_{in} are the output and input field amplitudes, respectively. As shown in Fig. 6, where coupling constants α and β are taken to be equal and losses are taken to be $\gamma_A = \gamma_B = \beta/10$, small variation of the resonant frequencies ω_A and ω_B leads to dramatic change in the bandwidth of the system. Such variation can be accomplished by modulating the refractive index in the cavity region. When cavity A has a much lower resonance frequency than that of cavity B, the lower-frequency eigenstate of the system has the characteristic of cavity A, with a broad bandwidth due to its coupling to the waveguides [Fig. 6(a), left panel]. The energy of such a state is strongly localized in the cavity A [Fig. 6(a), right panel]. On the other hand, when cavity B has a much lower resonance frequency than that of cavity A, the lower-frequency eigenstate exhibits a narrow transmission peak, characteristic of cavity B that is weakly coupled to the waveguide modes [Fig. 6(b), left panel]. And the eigenstate's energy is strongly localized in the cavity B [Fig. 6(b), right panel]. Small modulations of the resonant frequencies thus lead to strong modulations of the bandwidth of the system.

B. Caterpillar resonator system

To obtain a system with information storage capacity, we cascade the basic building block in Fig. 5 in a translationally invariant configuration as shown in Fig. 7 to generate a periodic array of cavities. Each unit cell of the periodic array contains a waveguide cavity A, which is coupled to the nearest-neighbor unit cells to form a coupled resonator optical waveguide, and one or more side cavities B_1 and B_2, which couples only to the cavities in the same unit cell. The side cavities in adjacent unit cells are placed in an alternating geometry in order to prevent direct coupling between them. This system is an example of the general scheme in Fig. 2, where each set of ith side cavities B_i forms a subsystem with very narrow bandwidth by themselves, and the waveguide cavities A form a subsystem with large bandwidth.

The band structure of such a system consists of two bands $\omega_{\pm,k}$ (Fig. 8) [26], and we focus on the lower band $\omega_{-,k}$, which has a group velocity at the band center of

$$\begin{aligned} v_{g-} &= \mathrm{Re}\left[\frac{d\omega_{-,k}}{dk}\right]_{k=\pi/2\ell} \\ &= \alpha\ell\,\mathrm{Re}\left[1-\frac{\Delta+i(\gamma_A-\gamma_B)}{\sqrt{[\Delta+i(\gamma_A-\gamma_B)]^2+4\beta^2}}\right] \end{aligned} \tag{4}$$

with $\Delta \equiv \omega_A - \omega_B$. When $\Delta \ll -|\beta|$, the lower band exhibits the characteristics of the waveguide cavities, and thus has a large group velocity ($v_g \simeq 2\alpha\ell$) and a large bandwidth [Fig. 8(a)]. The bandwidth of the lower system eigenstate decreases as ω_B is reduced and ω_A is increased [Fig. 8(b)]. When $\Delta \gg |\beta|$ [Fig. 8(c)], the lower band exhibits the characteristic of the side cavities with extremely narrow bandwidth, and the group velocity at the band center (and also the bandwidth) is reduced by a ratio of

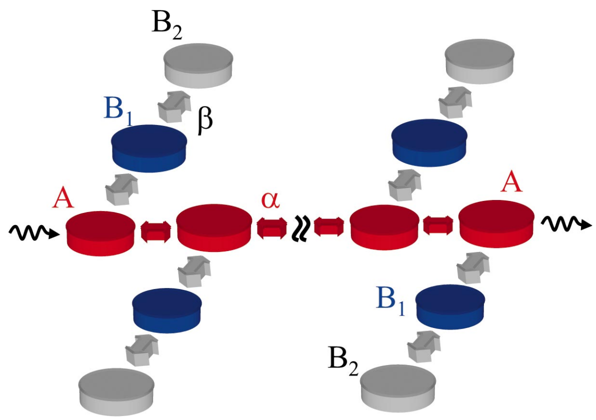

FIG. 7. (Color) Schematic of a tunable microcavity system used to stop light. The system consists of a periodic array of coupled Fano resonances shown in Fig. 5. Each unit cell of the array contains a waveguide cavity A, which couples to nearest-neighbor cells via evanescent coupling with a coupling strength α. Each waveguide cavity A is also coupled to either one or more side cavities. The coupling strengths between the waveguide cavities and the side cavities, and among the side cavities themselves, are labeled β_i. The figure shows the case with two side cavities, labeled as B_1 and B_2.

$$\left(\frac{\beta}{\Delta}\right)^2 + \frac{(\gamma_A - \gamma_B)^3}{4\Delta^3}. \qquad (5)$$

Importantly, the bandwidth reduction ratio and the group velocity become independent of loss when γ_A and γ_B are equal, which can be adjusted externally. Also, by increasing the number of side cavities in each unit cell as shown in Fig. 7, the minimum achievable group velocity at the band center can be further reduced to $2\alpha\ell\Pi_{i=1}^{r}(\beta_i/\Delta)^2$, where r is the number of the side cavities in each unit cell, and β_i is the coupling constant between the $(i\text{-}1)$th and ith side cavities as shown in Fig. 7. Thus, the group velocity can be reduced exponentially with linear increase in system complexity, and significant group velocity tuning can be accomplished with the use of small refractive index variation that changes the resonant frequencies ω_A and ω_B.

In this system, a pulse can be stopped by the following dynamic process: We start with $\Delta \ll -|\beta|$, such that the lower band has a large bandwidth. By placing the center of $\omega_{-,k}$ at the pulse carrier frequency ω_0 [Fig. 8(a)], the lower band can accommodate the entire pulse, with each spectral component of the pulse occupying a unique wave vector. After the pulse is completely in the system, we vary the resonance frequencies until $\Delta \gg |\beta|$ [Fig. 8(c)], at a rate that is slow enough compared with the frequency separation between the lower and the upper bands. [The frequency separation reaches a minimum value of $2|\beta|$ when $\Delta = 0$ as shown in Fig. 8(b) at the anticrossing point]. Assuming a constant and equal rate of change in the cavity resonance frequencies with $r \equiv d\Delta/dt$, the system can be described with the Landau-Zener model, and the probability of scattering from one of the eigenstates to the other eigenstate is equal to $P_{scat} = \exp[-2\pi\beta^2/r]$ [39]. The modulation of the cavity resonances preserves translational symmetry of the system. Therefore, cross talk between different wave-vector components of the pulse is prevented during the entire tuning process as indicated by the red dashed lines in Fig. 8. Also, the slow modulation rate ensures that each wave-vector component of the pulse follows only the lower band $\omega_{-,k}$, with negligible scattering into the upper band $\omega_{+,k}$ (i.e., the system evolves in an adiabatic [31] fashion). Consequently, the pulse bandwidth is revers-

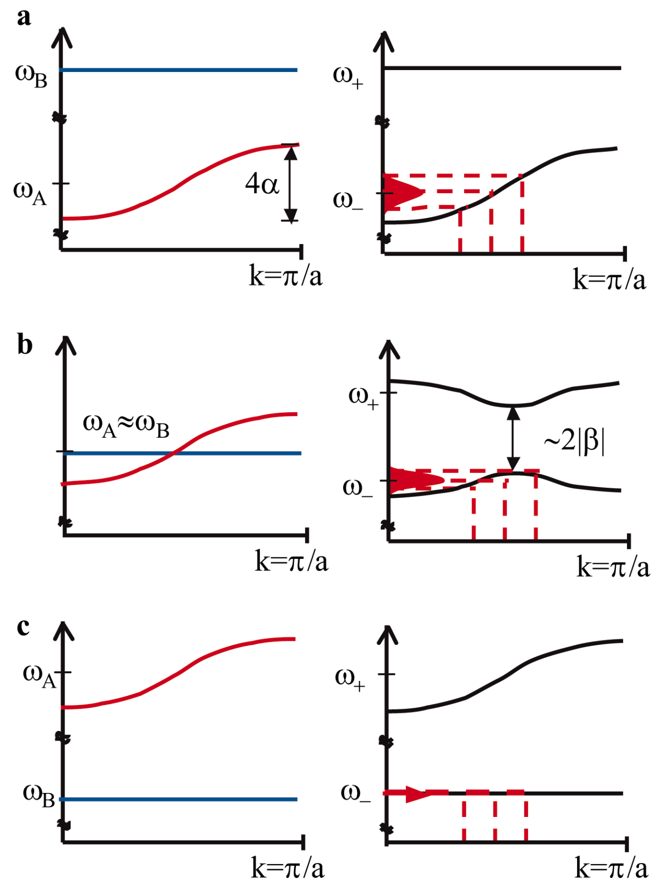

FIG. 8. (Color) Schematic of the frequency bands ω_+ and ω_- for the system shown in Fig. 6 with a single side cavity in each unit cell. ω_A and ω_B are the resonance frequencies for the waveguide cavities A and the side cavities B, respectively, and k is the wave vector. In the left panels, the red and blue curves correspond to the bands for the side cavities A and B by themselves, respectively. The waveguide cavities A are coupled to each other and thus the red curve has a large bandwidth. The side cavities B are not coupled to each other and thus the blue curve has zero bandwidth. The right panels are the band structures for the coupled system. The figure includes three cases. (a) $\omega_A - \omega_B \ll -|\beta|$. The lower-frequency band ω_- exhibits the characteristic of the subsystem of waveguide cavities A with a large bandwidth, and it is centered at the pulse frequency ω_0 to accept an incoming pulse with large bandwidth. (b) $\omega_A \approx \omega_B$. The waveguide cavities A and the side cavities B are near-resonant. The upper and lower bands on the right display a mixed character of both subsystems of waveguide cavities A and side cavities B. Here, the distance between the upper and lower bands is near its minimum $(\omega_{-,k} - \omega_{+,k} \approx 2|\beta|)$. (c) $\omega_A - \omega_B \gg |\beta|$. The lower-frequency band ω_- exhibits the characteristic of the subsystem of side cavities B with a very narrow bandwidth. Axes are in arbitrary units.

ibly compressed via energy exchange with the modulator, while all the information encoded in the pulse is preserved. An implementation of this dynamic system in photonic crystals has been computationally demonstrated previously [26].

C. A practical three-stage system

In practical optoelectronic devices [40], one can achieve index modulation strengths $(\delta n/n)$ on the order of 10^{-4} at a maximum speed exceeding 10 GHz with intrinsic electro-optic effects in bulk GaAs. Since such modulation strength is far weaker compared with what is used here in the FDTD simulation, the coupled-mode theory should apply even more accurately in the realistic situation. Therefore, using coupled-mode theory, we have simulated the structure shown in Fig. 7 with the two side cavities coupled to each waveguide cavity. We use coupling constants of $\beta_1 = 10^{-5}\ \omega_A$ and $\beta_2 = 10^{-6}\ \omega_A$, a maximum index shift of $\delta n/n = 10^{-4}$, and we assume a cavity loss rate of $\gamma = 4\times 10^{-7}\ \omega_A$ that has been measured in on-chip microcavity structures [41]. A waveguide-cavity coupling constant of $\alpha = 10^{-5}\ \omega_A$ is used to accommodate a 1 ns pulse. In this system, the process of energy transfer between multiple subsystems (Fig. 2) occurs in two stages [Fig. 9(a)]. First, the field is transferred from the cavities A to B_1, and the group velocity is reduced from its speed of 100 km/s (as limited by the bandwidth-delay product for a 1 ns pulse) to 1 km/s. Since the coupling constant between the cavities A and B_1 is large, this first bandwidth-compression process can be done rather rapidly within a time duration of a few nanoseconds without violating the adiabaticity condition. At the end of the process, the field localizes at the side cavities B_1. The next bandwidth compression stage occurs between cavities B_1 and B_2. Here, the modulation speed is slowed down when cavities B_1 and B_2 reach resonance near $t = 4t_{pass}$ [when the frequency difference between the eigenstates reaches a minimum of β_2 as shown in Fig. 8(b)] in order to obey adiabaticity, and then the modulation can be accelerated again as the separation between the resonance frequencies increases. At the end of this compression process, the group velocity reduces to below 10 cm/s. The use of three side cavities in the above example would decrease the speed of light down to 10 μm/s using a coupling constant β_3 equal to $\beta_2 = 10^{-6}\ \omega_A$. The group velocity decreases exponentially with a linear increase in the number of side-cavity stages, as explained earlier. Thus, there is no limit on the achievable minimum speed of light for a pulse with a finite initial bandwidth in practical physical systems. The same process repeated in reverse recovers the original pulse shape without any distortion at $t = 14.5t_{pass}$ in spite of the significant loss present. Thus the bandwidth compression mechanism is very robust against loss. If the cavity lifetime is improved only to a microsecond, nearly 99% of the original pulse energy can be recovered. At such ultraslow speeds, the pulses stay stationery in the side cavities and experience negligible forward propagation. The storage times then become limited only by the cavity lifetimes. Importantly, the storage times are also independent of the pulse bandwidths, which enable the use of ultrahigh quality-factor microcavities to store short (large bandwidth) pulses coherently, by overcoming the fundamental bandwidth constraints in ultrahigh Q cavities.

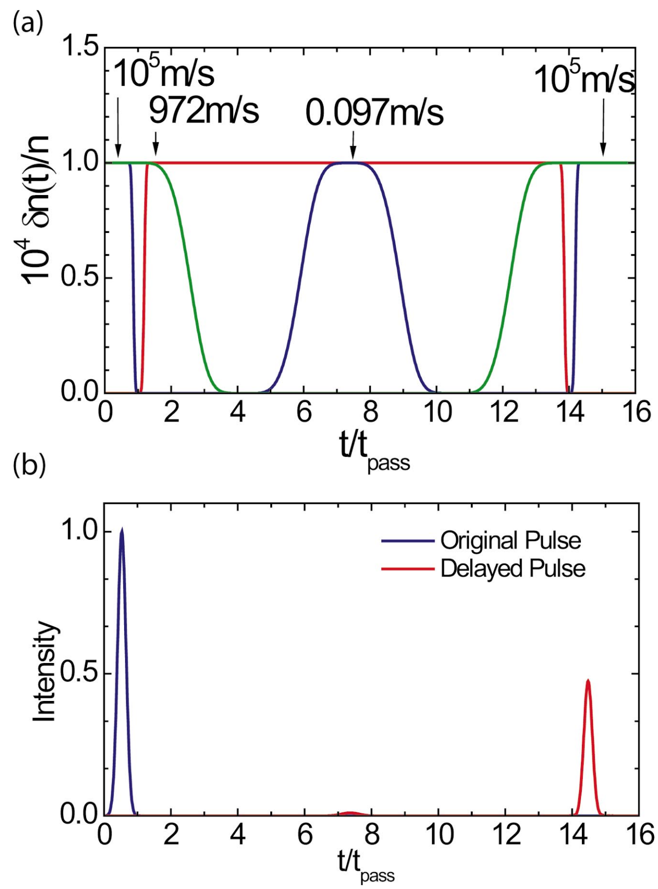

FIG. 9. (Color) Coupled mode theory simulation of a two-stage system with loss. The system is shown in Fig. 7. The losses of the cavities are taken from the measured losses in integrated on-chip microcavities [34]. (a) The red, blue, and green lines represent the relative changes in the refractive indices of the cavities A, B, and C, respectively, as a function of time. The group velocities of the pulse at several instances are also provided. (b) The blue line represents the incident pulse intensity in arbitrary units as recorded in the first waveguide cavity. The red line represents intensity as recorded in the last waveguide cavity, after the dynamical index tuning processes shown in (a).

D. General scaling analysis

Below we provide detailed discussion of our scheme given the constraints on optical losses and available index modulation strengths. The operating bandwidth of our system is limited by the strength of index modulations available. A system can accommodate a pulse with a bandwidth no greater than the largest system bandwidth. To compress the bandwidth of such a pulse to zero, the largest frequency shift $\delta\omega$ required is thus comparable to the largest system bandwidth. On the other hand, the largest frequency shift that can be accomplished for a given index modulation is $\omega\delta n/n$, where ω is the center frequency of the pulse. Therefore, the operating bandwidth of the system is on the order of

$$\delta\omega \sim \omega\delta n/n. \tag{6}$$

Since the pulses can be stopped before they propagate long distances, dispersion is not too critical, and a large portion of the system bandwidth can be utilized. For a small refractive index shift of $\delta n/n = 10^{-4}$, and assuming a carrier frequency of approximately 200 THz, as used in optical communications, the achievable bandwidth is comparable to the bandwidth of a single wavelength channel (20 GHz) in high-speed optical systems. In comparison, the atomic stop-light schemes have experimentally demonstrated bandwidths of less than 100 kHz [21–24]. The all-optical scheme thus represents a great improvement in the bandwidth of a light pulse that can be stopped.

The bandwidth compression process requires a finite number of cavities. The required system dimensions are determined by the spatial length of the pulse in the waveguide and by the duration of the modulation primarily during the first stage of the field transfer. Together, these two factors set the total distance L that the pulse travels before its initial speed v_{g0} is reduced significantly:

$$L \sim v_{g0}\tau_{pulse} + v_{g0}\tau_{mod}. \tag{7}$$

Since the minimum initial group velocity $v_{g0}(=2\alpha\ell)$ is proportional to the signal bandwidth $(\sim 4\alpha)$, and since the pulse duration τ_{pulse} is inversely proportional to the initial signal bandwidth, the first term on the rightmost side of Eq. (7) is approximately a constant independent of the signal bandwidth (e.g., $L \sim 10\ell + v_{g0}\tau_{mod}$). The second term can be minimized by using the smallest modulation rise time allowed within the adiabaticity constraint. Thus the first-stage coupling constant β_1 should be made large in order that fast tuning can be performed while still satisfying adiabaticity during modulation. Once the initial slowdown is accomplished, the pulse moves at a far slower speed, and does not change its shape as it comes to a halt. Thus the modulation in the subsequent stages can be made a lot slower, allowing the use of much smaller coupling constants in subsequent stages to accomplish further dramatic slowdown. Taking all these considerations into account, for a signal bandwidth of about 10 GHz, and a modulation rise time of 0.1 ns achievable in electro-optic systems, about 100 cavity pairs would be sufficient. Thus chip-scale implementation of such systems for large bandwidth signals is foreseeable.

In this particular system, the achievable maximum group velocity reduction is related to the coupling constant between the cavities and scales exponentially with the number of side cavities, and thus it is unlimited in principle. However, the time duration in which the bandwidth compression process should occur is limited by the optical loss rate γ if a significant part of the pulse energy should be preserved. Because of the adiabaticity requirement, this constraint on the minimum pulse compression duration determines the maximum number of subsystem stages η and the minimum coupling constants β_i between these stages. Accordingly, let us assume that the total modulation duration is an order of magnitude smaller than the cavity decay time to prevent losses, and that the secondary subsystem coupling rates are all equal $(\beta_i = \beta)$ and an order of magnitude larger than the modulation rate to satisfy adiabaticity. Then, coupling constants β should be roughly on the order of $\eta\gamma$. Since the reduction ratio of the group velocity is $(\beta/\Delta)^{2\eta} \approx (\eta\gamma/\Delta)^{2\eta}$, we minimize this ratio with respect to the number of stages η, and obtain $\eta = \Delta/\gamma e$, which represents the optimal number of stages needed for maximum group velocity reduction in the presence of losses. In addition to the group velocity reduction ratio, the minimum achievable group velocity is also determined by the initial group velocity of the pulse $(2\alpha\ell)$, which is related to the pulse bandwidth through the bandwidth-delay product. Combining these two factors, we have

$$v_g = 2\alpha\ell \prod_{i=1}^{r} (\beta_i/\Delta)^{\Delta/\gamma e}. \tag{8}$$

Taking into account both effects, we can obtain a total group velocity reduction much below 1 Å per hour for a 10 GHz bandwidth pulse without the pulse being attenuated even in the presence of lossy cavities with quality factors of 10^7. These estimates show that in these systems, even in the presence of losses, the pulses can essentially be stopped for all practical purposes.

V. CONCLUDING REMARKS

There are several potential applications for the all-optical bandwidth modulation and stopping light schemes. Multiple pulses can be held simultaneously in the system, and desired pulses can then be released on demand. This capability might enable controlled entanglement of networks of quantum systems in distant microcavities via photons, thus opening up the possibility of chip-scale photonic quantum information processing. We further note that the technique of coherent field transfer between multiple systems (Fig. 2) can be used to combine all-optical systems and atomic systems to overcome some of the fundamental bandwidth and wavelength limitations in the atomic systems. For example, the first few subsystems of such a system can be all-optical resonators with a large bandwidth to accommodate a fast optical pulse, and the last subsystem can consist of nuclear spin states with long lifetimes to store the electromagnetic coherence.

The loss in optical resonator systems might be counteracted with the use of gain media in the cavities [42], or with external amplification. Such capabilities could be important for the use of such schemes in optical communication systems. The loss in principle can also be suppressed with the use of three-dimensional photonic crystals. In such 3D crystals, the loss is only limited by intrinsic material losses. By using high-quality semiconductors or insulators, and by operating at a wavelength below the mid electronic band gap, the material loss might be quite low, and one might speculate that the lifetime of optical resonators might eventually exceed that of atomic resonances. For example, the material loss lifetime in fused silica is in fact on the order of 10^{-3} s, and cavity quality factors $(Q \simeq 8 \times 10^9)$ approaching this limit have already been measured in quartz microspheres [43]. Furthermore, optical modes with quality factors approaching 5×10^8 with large spectral spacing have also been demonstrated in integrated resonators [44]. With such long lifetime resonators, optical pulses can be stopped for durations sufficient for quantum information processing purposes. Development of even lower loss materials than silica without the requirement of making a fiber is also foreseeable.

The ultralow group velocity and bandwidth compression also dramatically enhances nonlinear effects over the entire bandwidths of pulses. This can enable single-photon quantum gates using instantaneous nonlinearities below the mid-band-gap of electronic systems. Since such nonresonant nonlinearities are practically decoherence-free, decoherence-free on-chip quantum computing at room temperature might be accomplished.

Since the required index of modulation is quite small, one can use the intrinsic nonresonant electro-optical effects in semiconductors to tune the refractive index, without using any lossy resonant electronic excitations. The side cavities where the photons are held ideally should possess a very large quality factor. In our scheme, such side cavities do not need to be modulated, and it is sufficient to modulate only the waveguide cavities. Thus, electrical contacts can be placed far away from the cavities that have high-quality factors. One might be able to further isolate the cavities from the electrical contacts with the use of fringing electric fields. Slight inaccuracies in microcavity resonance frequencies due to fabrication tolerances can be compensated by the built-in index tuning.

Using the few underlined basic principles above, it should be possible to stop light pulses in a wide variety of different physical systems, and the underlying ideas and schemes presented here are valid for all wave phenomena, including acoustics and microwave signals. Finally, the general scheme we presented can be used not only to stop light but also to completely reshape its spectrum while the photon pulse is in the system, leading to novel information-processing capabilities.

ACKNOWLEDGMENTS

This work was supported in part by NSF Grant No. ECS-0200445, and by the Packard Foundation. The simulations were performed at the Pittsburgh Supercomputing Center through the support of a NSF-NRAC grant. M.F.Y. acknowledges the support of Stanford University. The authors also acknowledge Professor Steve Harris at Stanford University for discussions.

[1] R. Ramaswami and K. N. Sivarajan, *Optical Networks: A Practical Perspective* (Morgan Kaufmann, San Francisco, CA, 1998).
[2] M. D. Lukin and A. Imamoglu, Nature (London) **413**, 273 (2001).
[3] L. M. Duan, M. D. Lukin, J. I. Cirac, and P. Zoller, Nature (London) **414**, 413 (2001).
[4] M. Fleischhauer and M. D. Lukin, Phys. Rev. A **65**, 022314 (2002).
[5] D. A. Braje, V. Balic, G. Y. Yin, and S. E. Harris, Phys. Rev. A **68**, 041801(R) (2003).
[6] L. Brillouin, *Wave Propagation and Group Velocity* (Academic, New York, 1960).
[7] S. E. Harris, Phys. Today **50**(7), 36 (1997).
[8] M. Kozuma, D. Akamatsu, L. Deng, E. W. Hagley, and M. G. Payne, Phys. Rev. A **66**, 031801(R) (2002).
[9] M. S. Bigelow, N. N. Lepeshkin, and R. W. Boyd, Phys. Rev. Lett. **90**, 113903 (2003).
[10] K. J. Boller, A. Imamoglu, and S. E. Harris, Phys. Rev. Lett. **66**, 2593 (1991).
[11] A. Kasapi, M. Jain, G. Y. Yin, and S. E. Harris, Phys. Rev. Lett. **74**, 2447 (1995).
[12] L. V. Hau, S. E. Harris, Z. Dutton, and C. H. Behroozi, Nature (London) **397**, 594 (1999).
[13] M. M. Kash *et al.*, Phys. Rev. Lett. **82**, 5229 (1999).
[14] D. Budker, D. F. Kimball, S. M. Rochester, and V. V. Yashchuk, Phys. Rev. Lett. **83**, 1767 (1999).
[15] N. Stefanou and A. Modinos, Phys. Rev. B **57**, 12127 (1998).
[16] A. Yariv, Y. Xu, R. K. Lee, and A. Scherer, Opt. Lett. **24**, 711 (1999).
[17] M. Bayindir, B. Temelkuran, and E. Ozbay, Phys. Rev. Lett. **84**, 2140 (2000).
[18] M. Notomi *et al.*, Phys. Rev. Lett. **87**, 253902 (2001).
[19] M. D. Lukin, S. F. Yelin, and M. Fleischhauer, Phys. Rev. Lett. **84**, 4232 (2000).
[20] M. Fleischhauer and M. D. Lukin, Phys. Rev. Lett. **84**, 5094 (2000).
[21] C. Liu, Z. Dutton, C. H. Behroozi, and L. V. Hau, Nature (London) **409**, 490 (2001).
[22] D. F. Phillips, A. Fleischhauer, A. Mair, R. L. Walsworth, and M. D. Lukin, Phys. Rev. Lett. **86**, 783 (2001).
[23] A. V. Turukhin *et al.*, Phys. Rev. Lett. **88**, 023602 (2002).
[24] M. S. Bigelow, N. N. Lepeshkin, and R. W. Boyd, Science **301**, 200 (2003).
[25] M. Bajcsy, A. S. Zibrov, and M. D. Lukin, Nature (London) **426**, 638 (2003).
[26] M. F. Yanik and S. Fan, Phys. Rev. Lett. **92**, 083901 (2004).
[27] G. Lenz, B. J. Eggleton, C. K. Madsen, and R. E. Slusher, IEEE J. Quantum Electron. **37**, 525 (2001).
[28] Z. Wang and S. Fan, Phys. Rev. E **68**, 066616 (2003).
[29] M. O. Scully and M. S. Zubairy, *Quantum Optics* (Cambridge University Press, Cambridge, 1997).
[30] The translational symmetry will be broken if there is a disorder in the system. However, the bandwidth compression process may not be significantly affected if the strength of the disorder is far smaller than the initial bandwidth of the system. A disorder would create a nonpropagating localized state with zero group velocity. Thus, the bandwidth-compressed pulse would still be localized within the system, although it will be reshaped due to disorder.
[31] A. Messiah, *Quantum Mechanics* (Interscience, New York, 1963).
[32] G. Juzeliunas and H. J. Carmichael, Phys. Rev. A **65**, 021601(R) (2002).

[33] K. Vahala, Nature (London) **424**, 839 (2003).
[34] E. Yablonovitch, Phys. Rev. Lett. **58**, 2059 (1987).
[35] S. John, Phys. Rev. Lett. **58**, 2486 (1987).
[36] J. D. Joannopoulos, R. D. Meade, and J. N. Winn, *Photonic Crystals: Molding the Flow of Light* (Princeton University Press, Princeton, NJ, 1995).
[37] S. Fan, Appl. Phys. Lett. **80**, 908 (2002).
[38] H. A. Haus, *Waves and Fields in Optoelectronics* (Prentice-Hall, Englewood Cliff, NJ, 1984).
[39] B. M. Garraway and K. A. Suominen, Rep. Prog. Phys. **58**, 365 (1995).
[40] S. L. Chuang, *Physics of Optoelectronic Devices* (Interscience, New York, 1995).
[41] D. K. Armani, T. J. Kippenberg, S. M. Spillane, and K. J. Vahala, Nature (London) **421**, 925 (2003).
[42] Y. Xu, Y. Li, R. K. Lee, and A. Yariv, Phys. Rev. E **62**, 7389 (2000).
[43] D. W. Vernooy, V. S. Ilchenko, H. Mabuchi, E. W. Streed, and H. J. Kimble, Opt. Lett. **23**, 247 (1998).
[44] K. Vahala, *Optical Microcavities* (World Scientific, New Jersey, 2004).